N-Doped Activated Carbons from Polypyrrole – Effect of Steam Activation Conditions

Juan J. Villora-Picó, M. Mercedes Pastor-Blas, and Antonio Sepúlveda-Escribano*

Dedicated to Prof. Dr. rer. nat. Jürgen Caro on the occasion of his 70th birthday

Polypyrrole (PPy) has been prepared by oxidative polymerization of pyrrole and used as a raw material for the preparation of N-doped activated carbons. Thus, PPy has been pyrolyzed at 900 °C and then activated with steam under different activation conditions (time and temperature). This has allowed for the preparation of activated carbons with different porosity development and nitrogen content, as well as distinctive distribution of nitrogen species. It has been observed that the presence of nitrogen functionalities favors water adsorption at low relative pressures but, at relative pressures higher than 0.5 it is determined by the porosity development.

Keywords: N-doped carbons, Polypyrrole, Steam activation, Water adsorption, XPS

1 Introduction

Activated carbons are materials characterized by having a high surface area and developed porosity. Their interesting properties, along with their low price and the variety of possible carbon precursors, make activated carbons the most widely used materials for adsorption of wastes and pollutants [1] as well as support in heterogeneous catalysts [2]. Activated carbons can be obtained from biomass raw materials such as olive stones [3], rice husk [4], corn cobs [5], etc. The porous structure is generated during the pyrolysis process, but most often it is necessary to submit the pyrolyzed material to an activation process to increase their surface area and to develop a more porous structure, what is required for most applications. Chemical activation treatments with activating agents such as phosphoric acid, $ZnCl_2$ and KOH require a post-treatment washing producing a large amount of contaminated water, which is an environmental issue. Alternative physical (thermal) activation treatments based on carbon gasification with CO_2 or steam do not produce solid or liquid wastes, being the main by-products CO, CO_2 and H_2 [6, 7], what eliminates the need for a post-activation cleaning process. The chosen activating agent determines the type of porosity developed. Carbons activated with CO_2 mainly show micropores whereas steam activation treatments develop micro- and mesoporosity [8, 9].

For different applications it is also important to assure a good carbon-adsorbate interaction, and this can be achieved by the incorporation of heteroatoms to the carbon structure [10]. In this sense, the use of phosphorous [11], sulfur [12], boron [13, 14], and nitrogen [15, 16] as carbon dopants has

been reported. In particular, it has been shown that doping with nitrogen atoms enhances the ability to adsorb non-polar or weakly polar molecules such as toluene [17]. Similar results were obtained by Shen et al. [18], who showed that the basicity imparted by N-doping improves the interaction with the aromatic electron ring of toluene.

Besides volatile organic compounds (VOCs) adsorption [18, 19], many other applications of doped carbons have been reported. They have been used in fuel cells for the oxygen reduction reaction [20–23], as electrodes for electric double-layer capacitors [24] or capacitive deionization [25, 26], as electrocatalysts in the methanol [27] or formic acid [28] oxidation reaction, as catalysts supports in hydrogenation reactions [15, 29] and in the Knoevenagel condensation reaction [30], among others.

N-doping can be achieved in several ways. A thermal treatment with ammonia results in the doping of the carbon surface. However, the bulk remains unmodified. The physical mixing of a previously prepared activated carbon with a compound with high nitrogen content such as melamine, followed by a pyrolysis treatment, results in the incorporation of nitrogen atoms in the carbon matrix. It is also possible to use N-containing polymers such as polyacrylonitrile [31], polyaniline [32] or polypyrrole [33] as carbon precur-

Juan J. Villora-Picó, M. Mercedes Pastor-Blas, Antonio Sepúlveda-Escribano
asepul@ua.es
Universidad de Alicante, Departamento de Química Inorgánica – Instituto Universitario de Materiales de Alicante (IUMA), Apartado 99, 03080 Alicante, Spain.

sors. As these polymers already have nitrogen atoms in their structure, the resulting activated carbons show a good distribution of N in both the bulk and the surface. Besides, it is possible to control the experimental variables such as temperature and time of the pyrolysis and activation treatments to tailor the desired final properties of the N-doped carbons.

Depending on the targeted application of a given activated carbon, its ability for water adsorption can be considered as a problem or as a sought-after feature. Thus, it is a problem in gas streams purification, especially when dealing with VOCs such as benzene or toluene, the adsorption of which can be hampered by the presence of water [34]. On the other hand, water adsorption is a desirable process in applications related with adsorption heat pumps [35]. Although the surface of activated carbons is inherently hydrophobic, the presence of functional groups (e.g., oxygen functional groups) and/or defect sites can favor water adsorption at low humidity, as they act as anchoring sites for water molecules, that then grow as a cluster as humidity increases. In this sense, water adsorption at low humidity (or relative pressure) can be used as an indication of the amount of surface functional groups in activated carbons. At high humidity levels it? is the porosity development, which determines both the adsorption capacity and the wideness of the hysteresis loop [36].

In addition to oxygen surface functional groups, some works have reported that nitrogen functionalities can also affect the water adsorption behavior of activated carbons. Matsuoka et al. studied N-doped carbon aerogel and observed that water uptake was improved by the presence of nitrogen atoms, in such a way that it increased at low pressures with the nitrogen content [37]. These results were confirmed by Harikawa et al. [38], who also observed that the saturated amount adsorbed depended on the pore size, which determines the packing ability of water molecules.

In this work, polypyrrole has been synthesized and used as the source of nitrogen and precursor of the activated carbons. Different preparation variables such as temperature and time have been considered during the pyrolysis and the steam activation treatments, and the properties of the obtained materials have been assessed and discussed as a function of the preparation variables. Furthermore, the ability of the prepared activated carbons for water adsorption at 25 °C has been assessed.

2 Experimental

Polypyrrole (PPy) was prepared by the oxidative polymerization of the pyrrole monomer (C_4H_5N, M = 67.09 g mol^{-1}, density = 0.967 g mL^{-1}, purity 98 %, from Sigma Aldrich) using iron chloride hexahydrate ($FeCl_3 \cdot 6H_2O$, M = 270.3 g mol^{-1}, from Sigma Aldrich) as oxidant, in a molar ratio (oxidant:monomer) of 2.31:1. The oxidant (9 g) was dissolved in distilled water (200 mL) and then 1 mL of pyr-

role monomer was added drop-wise under constant magnetic stirring for 6 h at room temperature. The solution turned dark, indicating the progress of the polymerization reaction. The precipitated PPy polymer was then filtered from the solution and washed with distilled water until the washing water turned colorless. Finally, PPy was dried in an oven at 80 °C for 12 h.

For the preparation of the carbon materials, PPy was pyrolyzed in a tubular furnace under nitrogen flow (100 mL min^{-1}) at 900 °C, with a heating ramp of 5 °C min^{-1}. The obtained carbons were activated with steam at different temperatures and different lengths of time in a tubular furnace with a water flow of one drop every four minutes. The samples prepared were named as follows: PPy-pyrolysis temperature divided by 100-activation temperature divided by 100-activation time in hours. For instance, PPy-P8-S7-4 refers to a carbon obtained from PPy pyrolyzed at 800 °C and steam activated at 700 °C for 4 h.

The textural properties of the carbons were determined by N_2 and CO_2 adsorption at –196 °C and 0 °C, respectively, using an Autosorb-6 equipment (Quantachrome). The samples were previously outgassed at 250 °C for 4 h under vacuum in an Autosorb Degasser (Quantachrome).

X-ray photoelectron spectroscopy (XPS) allowed to characterize the surface chemistry of the prepared materials. The experiments were carried out in a K-alpha spectrometer (Thermo-Fischer Scientific) using the Al Kα monochromatic radiation (1486.6 eV) as X-ray source. The C 1s core level binding energy at 284.6 eV was used as the reference binding energy.

SEM images have been obtained with a Hitachi S3000N instrument equipped with an X-ray detector XFlash 3001 model for EDS and mapping.

Elemental analysis (CHNS) was assessed in a Microanalyser equipped with a detection system Micro TruSpec of LECO. This system uses He as carrier gas and contains an infrared detector and a thermal conductivity detector that simultaneously analyses carbon, hydrogen, nitrogen and sulfur.

Water adsorption isotherms were obtained with a Vstar Win instrument (Quantachrome) for water and organic vapors adsorption. Previous to the determination of the adsorption isotherms, samples were outgassed at 250 °C for 4 h under vacuum.

3 Results and Discussion

3.1 Textural Properties

Fig. 1 shows the N_2 adsorption-desorption isotherms at –196 °C for the pyrolyzed PPy (PPy P9) and the different activated carbons obtained from it by steam activation. From them, the textural parameters have been calculated, which are reported in Tab. 1. The pyrolysis treatment of PPy produces a nonporous carbon, PPy P9. Therefore, an
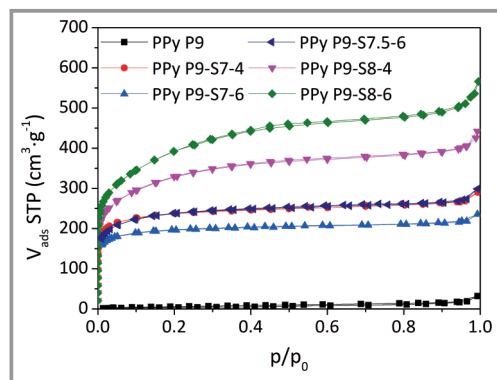
Figure 1. N_2 adsorption-desorption isotherms at $-196\,°C$.

Table 1. Textural parameters calculated from the N_2 adsorption-desorption isotherms at $-196\,°C$.

Sample	V_t [cm^{3}g^{-1}]	V_{micro} [cm^{3}g^{-1}]	V_{meso} [cm^{3}g^{-1}]	S_{BET} [m^{2}g^{-1}]
PPy P9	0.03	0.01	0.02	15
PPy P9-S7-4	0.42	0.35	0.07	907
PPy P9-S7-6	0.34	0.30	0.04	761
PPy P9-S7.5-6	0.42	0.35	0.07	891
PPy P9-S8-4	0.63	0.44	0.19	1184
PPy P9-S8-6	0.79	0.51	0.28	1407

activation treatment is mandatory to develop the porosity of this material. Steam activation results satisfactory in the development of the porosity and increasing surface area; however, it is affected by the experimental conditions such as temperature and time.

Carbons prepared by steam activation at 700 and 750 °C show type I isotherms, which are characteristic of microporous materials. The increase of the activation temperature to 800 °C produces the widening of the knee, as well as an increase of the plateau's slope, this indicating the formation of a more developed porosity, which also includes mesopores.

The specific surface areas, determined using the Brunauer-Emmet-Teller (BET) method, are reported in Tab. 1, as well as the micropore volume (V_{micro}) obtained from the application of the Dubinin-Raduschkevich (D-R) equation. The total pore volume (V_t) has been calculated from the amount adsorbed at a relative pressure of 0.95, and the mesopore volume is the difference between V_t and V_{micro}. Pore volumes are given as for liquid nitrogen at $-196\,°C$. It is clear that the increase of the activation temperature produces a strong increase in surface area and pore volumes. In fact, it can be seen that mesoporosity is not developed with activation below 800 °C. At this temperature, the longer the activation treatment, the higher surface area and porosity is achieved.

Microporosity was further assessed by comparing the micropore volumes obtained with N_2 adsorption at $-196\,°C$ and that obtained from CO_2 adsorption at $0\,°C$. In this sense, CO_2 adsorption isotherms at $0\,°C$ were obtained, and they are presented in Fig. 2. The CO_2 micropore volumes were obtained by application of the D-R model to the adsorption data; they are reported in Tab. 2 and compared to the micropore volumes obtained from N_2 adsorption. Since the critical dimension of both molecules are very similar (0.28 nm for CO_2 and 0.30 nm for N_2), the higher adsorption temperature for CO_2 facilitates the diffusion through the narrow micropores in which diffusion of nitrogen molecules is hindered. Thus, larger values for V_{micro} CO_2 than for V_{micro} N_2 indicates a very narrow porosity in which the adsorption equilibrium is more difficult to achieve for nitrogen adsorption at $-196\,°C$.
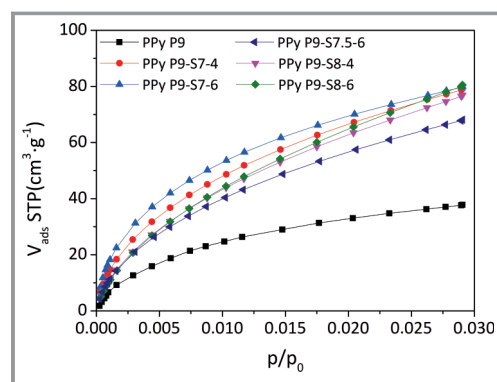

Figure 2. CO_2 adsorption-desorption isotherms at $0\,°C$.

Table 2. Textural parameters calculated from the N_2 and CO_2 adsorption isotherms.

Sample	V_{micro} N_2 [cm^{3}g^{-1}]	V_{micro} CO_2 [cm^{3}g^{-1}]
PPy P9	0.01	0.13
PPy P9-S7-4	0.35	0.25
PPy P9-S7-6	0.30	0.23
PPy P9-S7.5-6	0.35	0.21
PPy P9-S8-4	0.44	0.27
PPy P9-S8-6	0.51	0.28

It is worth noting that for the pyrolyzed sample (PPy P9) the micropore volume measured with CO_2 is larger than that obtained with N_2. This indicates that this sample contains a very narrow porosity in which nitrogen diffusion at $-196\,°C$ is hindered. Steam activation is useful to develop this incipient porosity, as can be seen with the evolution of the micropore volumes and the surface areas. For the steam activated samples, V_{micro} CO_2 is always smaller than V_{micro} N_2, what is expected if one takes into account the much

lower relative pressure at which the CO_2 adsorption isotherms are measured, which only cover the smaller micropores (less than 0.7 nm in size). However, nitrogen adsorption covers the whole porosity including micropores and also mesopores. It can be seen in Tab. 2 that the increase of the activation temperature produces an increase in both V_{micro} CO_2 and V_{micro} N_2. However, the effect is more important for the latter, indicating steam activation mainly produces the widening of porosity and favors the formation of mesopores.
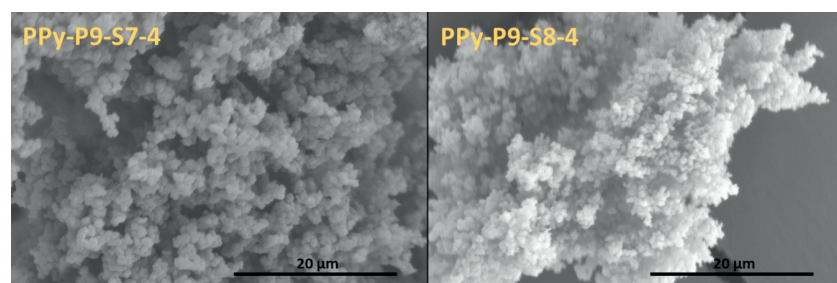
3.2 SEM Analysis

The morphology of the activated carbons, determined by SEM (Fig. 3) is mainly globular and consists of a conglomeration of irregular particles, which are smaller when the activation treatment is performed at the highest temperature.

3.3 Surface Chemistry Characterization

Adsorption and catalytic properties are highly dependent not only on the textural properties, but also on the surface functionalities of the activated carbon [10, 39]. In this work, the surface chemistry of the prepared activated carbons has been studied by XPS. Tab. 3 reports the surface atomic percentage of carbon, oxygen, and nitrogen for the different samples. It can be seen that the pyrolyzed material (PPy P9) contains the larger amount of surface nitrogen atoms. However, a part of it is lost during the steam activation treatment, especially at increased temperatures and longer activation times. Nevertheless, in all cases there is an effective incorporation of nitrogen into the carbon structure, which is always higher than 2 at %. The detected oxygen content is due to the partial oxidation of the carbon surface during the activation treatment.

A qualitative and quantitative analysis of the different nitrogen species on the carbons' surface was assessed from the curve fitting of the N 1s core level (Fig. 4, Tab. 4). Several nitrogen species with different contributions to the N 1s bend were found in the XPS spectra: pyridinic-N

Table 3. Atomic composition of the carbon surface, obtained by XPS.

Sample	C 1s [at %]	O 1s [at %]	N 1s [at %]
PPy-P9	90.0	2.2	7.8
PPy-P9-S7-4	87.4	5.4	7.2
PPy-P9-S7-6	85.9	9.7	4.2
PPy-P9-S7.5-6	88.9	7.0	4.2
PPy-P9-S8-4	91.5	4.9	3.6
PPy-P9-S8-6	93.6	4.1	2.3
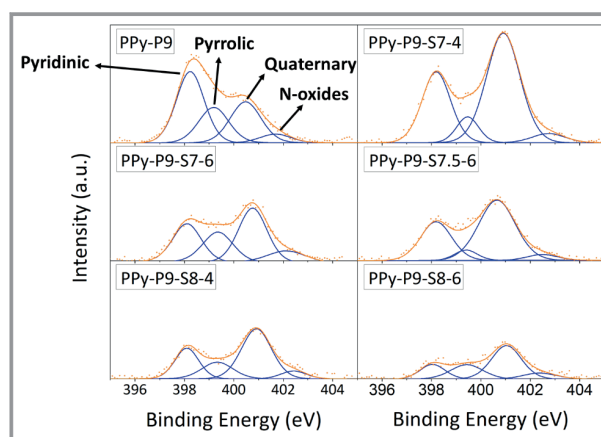
Figure 4. N 1s core level spectra deconvolution for the different samples.

($\approx$ 398 eV), pyrrolic-N ($\approx$ 399–400 eV), quaternary-N (($\approx$ 400–401 eV) and oxidized nitrogen ($\approx$ 402 eV) [40]. The relative amount of each species depends on the activation treatment. Whereas the parent pyrolyzed material contains mainly pyridinic-type nitrogen (43 at %), the quaternary-N contribution to the total N amount is predominant in the activated samples. This is in agreement with previous works reporting that treatments at high temperature favors the presence of quaternary nitrogen species, which have the highest thermal stability [41]. Quaternary nitrogen atoms replace carbon atoms in the graphene layers and, thus, greatly contribute to the modification of important properties of the carbons such as their electrical conductivity, and constitute anchoring sites that are able to stabilize metal particles when the carbons are used as catalysts supports.

3.4 Elemental Analysis

Whereas XPS analysis (Tab. 3) is restricted to the carbon surface, CHNS analysis (Tab. 5) provides information of

Figure 3. SEM images of PPy-P9-S7-4 and PPy-P9-S8-4, as representative of our PPy-based activated carbons.

Table 4. Nitrogen species obtained from the N 1s core level spectra deconvolution for the different samples.

Sample	Binding energy [eV]	[at %]	[%]
PPy-P9	398.2	3.36	43
	399.2	1.81	23
	400.5	2.14	28
	401.7	0.46	6
PPy-P9-S7-4	398.2	2.19	31
	399.5	0.62	9
	400.9	4.01	56
	402.8	0.33	4
PPy-P9-S7-6	398.1	1.19	27
	399.4	1.00	23
	400.8	1.70	39
	402.1	0.50	11
PPy-P9-S7.5-6	398.2	1.31	31
	399.4	0.26	6
	400.6	2.40	58
	402.5	0.20	5
PPy-P9-S8-4	398.1	0.88	24
	399.3	0.63	18
	400.9	1.82	51
	402.4	0.25	7
PPy-P9-S8-6	398.1	0.42	18
	399.4	0.53	23
	401.0	1.12	49
	402.4	0.23	10

Table 5. Atomic composition of the carbon surfaces obtained by CHNS.

Sample	C [%]	H [%]	O [%]	N [%]
PPy P9-S7-4	65.05	1.97	26.75	6.23
PPy P9-S8-4	71.22	1.66	24.11	3.01

the chemical composition of the bulk carbon. However, it can be seen that atomic nitrogen percentages obtained with both techniques are similar for the samples activated for 4 h at 700 °C, indicating a homogeneous dispersion of nitrogen thorough the samples.

3.5 Water Adsorption at 25 °C

Quaternary nitrogen, also referred as "graphitic nitrogen", is the nitrogen atom incorporated to the activated carbon structure by the replacement of a carbon atom and, as mentioned above, is the most thermally stable N species [41]. On the other hand, it has been reported that pyridinic- and pyrrolic-type nitrogen species have the ability of acting as basic sites on the carbon surface, and that the electronic density increases at quaternary nitrogen sites [42], what is highly interesting for catalytic and adsorption applications as this enhanced density may favor the interaction with polar molecules.

On the other hand, as it has been discussed above, water adsorption can be detrimental in applications where it can compete with other molecules for the active sites at the surface or for the available pore volume [43]. Therefore, water adsorption at 25 °C has been assessed on the prepared N-doped activated carbons to determine the possible effect of the presence of N-sites. The obtained adsorption isotherms are presented in Fig. 5. As expected, they are in all cases type V isotherms characteristic of a relatively weak interaction between the carbon surface and the adsorbate (water, in this case) although, in all cases, water adsorption starts already in the low relative pressure range, indicating the positive effect of nitrogen functionalities.
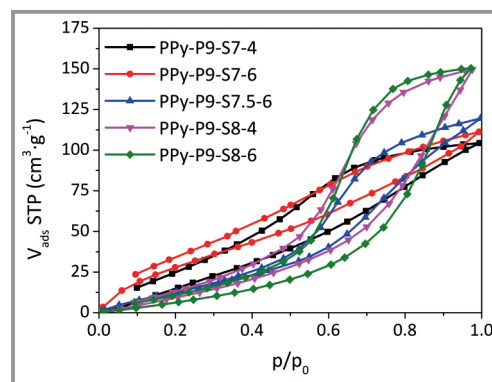
Figure 5. Water adsorption-desorption isotherms at 25 °C.

The amount adsorbed at low relative pressures clearly correlates with the amount of dopant nitrogen, as determined by XPS, being higher for samples activated under milder conditions. This is a proof of the role of nitrogen functionalities as anchoring centers for water molecules. It is also worth to note the important effect of the activation temperature in determining the shape of the adsorption-desorption isotherms, what is related to the development of porosity achieved at each temperature. Thus, samples activated at 800 °C show a faster enhancement of water adsorption as the partial pressure increases, with a wider hysteresis loop. This is assigned to their well-developed porosity that favors the package of adsorbed water molecules. It has been reported [44] that water adsorption at low pressures is due

to the presence of surface groups, whereas adsorption at high pressures is enhanced by a large pore volume. Furthermore, the adsorption mechanism is different depending on the type of porosity present in the activated carbon. When it is not properly developed, water adsorption is mainly determined by the number of active sites on which water molecules can anchor. In activated carbons with well-developed porosity, the growth of the initial cluster of water molecules is favored, and they can fill the pores with high packing efficiency. Thus, in samples such as those activated at 800 °C, water molecules firstly adsorb (at low relative pressures) on nitrogen sites forming 1D- and 2D- clusters; then, at relative pressures higher than about 0.5 the adsorption is dominated by the growth of 3D-clusters, which behave as a liquid. This is confirmed by the existence of the hysteresis loop [43].

Consequently, the activated carbon samples activated at 800 °C show an important water adsorption capability at high relative pressures, as a consequence of their well-developed porosity. Besides, the presence of nitrogen doping atoms, although in a relatively low amount, enhances the adsorption at low relative pressures. It can be concluded that these activated carbons are promising materials for applications such as adsorption heat pumps or desiccant humidity conditioners.

4 Conclusions

Nitrogen-doped activated carbons have been prepared by pyrolysis of polypyrrole (PPy) and activation of the resulting carbonized material with steam under different preparation conditions (temperature and time) have been performed. It has been shown that the activation conditions greatly affect the carbon properties, such as nitrogen content and porosity. In this sense, nitrogen content decreases as the activation temperature and/or time increases, due to the decomposition of the nitrogen functionalities. The distribution of different nitrogen species is also affected, being the quaternary nitrogen the most thermal stable one, thus prevailing after harsher activation conditions. It has been demonstrated that nitrogen functionalities favor water adsorption in the low-pressure range, what can be ascribed to the role of nitrogen atoms as anchoring sites for water molecules due to the important interaction among them. At high relative pressures (> 0.5), water adsorption is determined by the porosity development, which favors the packing of water molecules as 3D-clusters and thus, the best behavior is obtained with carbons prepared by activation at 800 °C, despite their lower nitrogen content.

References

[1] J. Saleem, U. Bin Shahid, M. Hijab, H. Mackey, G. McKay, *Biomass Convers. Biorefin.* **2019**, *9*, 775–802. DOI: https://doi.org/10.1007/s13399-019-00473-7

[2] F. Coloma, A. Sepúlveda-Escribano, J. L. G. Fierro, F. Rodriguez-Reinoso, *Appl. Catal., A.* **1996**, *148 (1)*, 63–80. DOI: https://doi.org/10.1016/S0926-860X(96)00218-9

[3] M. L. Martínez, M. M. Torres, C. A. Guzmán, D. M. Maestri, *Ind. Crops Prod.* **2006**, *23 (1)*, 23–28. DOI: https://doi.org/10.1016/j.indcrop.2005.03.001

[4] A. Amaya, N. Medero, N. Tancredi, H. Silva, C. Deiana, *Bioresour. Technol.* **2007**, *98 (8)*, 1635–1641. DOI: https://doi.org/10.1016/j.biortech.2006.05.049

[5] N. Bagheri, J. Abedi, *Chem. Eng. Res. Des.* **2009**, *87 (8)*, 1059–1064. DOI: https://doi.org/10.1016/j.cherd.2009.02.001

[6] Y. Wang, D. A. Bell, *Fuel* **2017**, *187*, 94–102. DOI: https://doi.org/10.1016/j.fuel.2016.08.109

[7] C. Schneider, M. Zeller, D. Böhm, T. Kolb, *Fuel* **2021**, *299*, 120523. DOI: https://doi.org/10.1016/j.fuel.2021.120523

[8] F. Rodríguez-Reinoso, M. Molina-Sabio, M. T. González, *Carbon* **1995**, *33 (1)*, 15–23. DOI: https://doi.org/10.1016/0008-6223(94)00100-E

[9] R. Arriagada, R. García, M. Molina-Sabio, F. Rodríguez-Reinoso, *Microporous Mater.* **1997**, *8 (3–4)*, 123–130. DOI: https://doi.org/10.1016/S0927-6513(96)00078-8

[10] Y. Du, H. Chen, X. Xu, C. Wang, F. Zhou, Z. Zeng, W. Zhang, L. Li, *Microporous Mesoporous Mater. A.* **2020**, *293*, 109831. DOI: https://doi.org/10.1016/j.micromeso.2019.109831

[11] J. Wu, C. Jin, Z. Yang, J. Tian, R. Yang, *Carbon* **2015**, *82*, 562–571. DOI: https://doi.org/10.1016/j.carbon.2014.11.008

[12] M. Sevilla, A. B. Fuertes, *Microporous Mesoporous Mater.* **2012**, *158*, 318–323. DOI: https://doi.org/10.1016/j.micromeso.2012.02.029

[13] L. Yang, S. Jiang, Y. Zhao, L. Zhu, S. Chen, X. Wang, Q. Wu, J. Ma, Y. Ma, Z. Hu, *Angew. Chem., Int. Ed.* **2011**, *50 (31)*, 7132–7135. DOI: https://doi.org/10.1002/anie.201101287

[14] Y. Lin, S. Wu, W. Shi, B. Zhang, J. Wang, Y. A. Kim, M. Endo, D. S. Su, *Chem. Commun.* **2015**, *51*, 13086. DOI: https://doi.org/10.1039/C5CC01963J

[15] J. J. Villora-Picó, I. Campello-Gómez, J. C. Serrano-Ruiz, M. M. Pastor-Blas, A. Sepúlveda-Escribano, E. V. Ramos-Fernández, *Catal. Sci. Technol.* **2021**, *11*, 3845–3854. DOI: https://doi.org/10.1039/D1CY00140J

[16] X. Ma, L. Li, Z. Zeng, R. Chen, C. Wang, K. Zhou, C. Su, H. Li, *Chem. Eng. J.* **2019**, *363*, 49–56. DOI: https://doi.org/10.1016/j.cej.2019.01.132

[17] L. Zeng, X. Li, S. Fan, J. Mu, M. Qin, X. Wang, G. Gang, M. Tade, S. Liu, *ACS Sustainable Chem. Eng.* **2019**, *7 (5)*, 5057–5064. DOI: https://doi.org/10.1021/acssuschemeng.8b05863

[18] Y. Shen, N. Zhang, *Environ. Res.* **2020**, *189 (5)*, 109956. DOI: https://doi.org/10.1016/j.envres.2020.109956

[19] C. Su, Y. Guo, H. Chen, J. Zou, Z. Zeng, L. Li, *Colloids Surf., A.* **2020**, *601*, 124983. DOI: https://doi.org/10.1016/j.colsurfa.2020.124983

[20] Z. Yang, H. Nie, X. Chen, X. Chen, S. Huang, *J. Power Sources* **2013**, *236*, 238–249. DOI: https://doi.org/10.1016/j.jpowsour.2013.02.057

[21] S. Zhang, W. Xia, Q. Yang, Y. V. Kaneti, X. Xu, S. M. Alshehri, T. Ahamad, Md. S. A. Hossain, J. Na, J. Tang, Y. Yamauchi, *Chem. Eng. J.* **2020**, *396*, 125154. DOI: https://doi.org/10.1016/j.cej.2020.125154

[22] H. Tan, J. Tang, J. Kim, Y. V. Kaneti, Y-M. Kang, Y. Sugahara, Y. Yamauchi, *J. Mater. Chem. A.* **2019**, *7*, 1380–1393. DOI: https://doi.org/10.1039/C8TA08870E

[23] T. Marshall-Roth, N. J. Libretto, A. T. Wrobel, K. J. Anderton, M. L. Pegis, N. D. Ricke, T. V. Voorhis, J. T. Miller, Y. Surendranath, *Nat. Commun.* **2020**, *11*, 5283. DOI: https://doi.org/10.1038/s41467-020-18969-6

[24] G. Hasegawa, M. Aoki, K. Kanamori, K. Nakanishi, T. Hanada, K. Tadanaga, *J. Mater. Chem.* **2011**, *21*, 2060–2063. DOI: https://doi.org/10.1039/C0JM03793A

[25] H. Zang, C. Wang, W. Zhang, M. Zhang, J. Qi, J. Qian, X. Sun, B. Yuliarto, J. Na, T. Park, H. G. A. Gomaa, Y. V. Kaneti, J. W. Yi, Y. Yamauchi, J. Li, *J. Mater. Chem. A.* **2021**, *9*, 12807–12817. DOI: https://doi.org/10.1039/D0TA10797B

[26] X. Xu, J. Tang, Y. V. Kaneti, H. Tan, T. Chen, L. Pan, T. Yang, Y. Bando, Y. Yamauchi, *Mater. Horiz.* **2020**, *7*, 1404–1412. DOI: https://doi.org/10.1039/C9MH01829H

[27] J. J. Fan, Y. J. Fan, R. X. Wang, S. Xiang, H. G. Tang, S. G. Sun, *J. Mater. Chem. A.* **2017**, *5*, 19467–19475. DOI: https://doi.org/10.1039/C7TA05102F

[28] Y. Xiong, J. Dong, Z. Q. Huang, P. Xin, W. Chen, Y. Wang, Z. Li, Z. Jin, W. Xing, Z. Zhuang, J. Ye, X. Wei, R. Cao, L. Gu, S. Sun, L. Zhuang, X. Chen, H. Yang, C. Chen, Q. Peng, C.-R. Chang, D. Wang, Y. Li, *Nat. Nanotechnol.* **2020**, *15*, 390–397. DOI: https://doi.org/10.1038/s41565-020-0665-x

[29] M. Tang, S. Mao, M. Li, Z. Wei, F. Xu, H. Li, Y. Wang, *ACS Catal.* **2015**, *5 (5)*, 3100–3107. DOI: https://doi.org/10.1021/acscatal.5b00037

[30] T. Tanabe, Y. Yamada, J. Kim, M. Koinuma, S. Kubo, N. Shimano, S. Sato, *Carbon* **2016**, *109*, 208–220. DOI: https://doi.org/10.1016/j.carbon.2016.08.003

[31] J. Zhu, C. Chen, Y. Lu, Y. Ge, H. Jiang, K. Fu, X. Zhang, *Carbon* **2015**, *94*, 189–195. DOI: https://doi.org/10.1016/j.carbon.2015.06.076

[32] T. Zhu, J. Zhu, Z. Li, S. Li, W. Si, S. Zhuo, *J. Mater. Chem. A.* **2014**, *2*, 12545–12551. DOI: https://doi.org/10.1039/C4TA01465K

[33] G. Xu, B. Ding, P. Nie, L. Shen, J. Wang, X. Zhang, *Chem. Eur. J.* **2013**, *19*, 12306–12312. DOI: https://doi.org/10.1002/chem.201301352

[34] J. Rodríguez-Mirasol, T. Cordero, J. J. Rodríguez, *Sep. Sci. Technol.* **2005**, *40 (15)*, 3113–3135. DOI: https://doi.org/10.1080/01496390500385277

[35] S. G. Wang, R. Z. Wang, X. R. Li, *Renewable Energy* **2005**, *30 (9)*, 1425–1441. DOI: https://doi.org/10.1016/j.renene.2004.10.012

[36] T. Horikawa, T. Sekida, J. Hayashi, M. Katoh, D. D. Do, *Carbon* **2011**, *49 (2)*, 416–424. DOI: https://doi.org/10.1016/j.carbon.2010.09.038

[37] T. Matsuoka, H. Hatori, M. Kodama, J. Yamashita, N. Miyajima, *Carbon* **2004**, *42 (11)*, 2329–2366. DOI: https://doi.org/10.1016/j.carbon.2004.04.031

[38] T. Harikawa, N. Skao, T. Sekida, J. Hayashi, D. D. Do, M. Katoh, *Carbon* **2012**, *50*, 1833–1842. DOI: https://doi.org/10.1016/j.carbon.2011.12.033

[39] R. Manjunatha, A. Karajic, M. Liu, Z. Zhai, L. Dong, W. Yan, D. P. Wilkinson, J. Zhang, *Electrochem. Energy Rev.* **2020**, *3*, 506–540. DOI: https://doi.org/10.1007/s41918-020-00069-0

[40] M. Ayiania, M. Smith, A. J. R. Hensley, L. Scudiero, J.-S. McEwen, M. García-Pérez, *Carbon* **2020**, *162*, 528–544. DOI: https://doi.org/10.1016/j.carbon.2020.02.065

[41] X. Duan, H. Sun, Y. Wang, J. Kang, S. Wang, *ACS Catal.* **2015**, *5 (2)*, 553–559. DOI: https://doi.org/10.1021/cs5017613

[42] E. Haque, J. W. Jun, S. N. Talapaneni, A. Vinu, S. H. Jhung, *J. Mater. Chem.* **2010**, *20*, 10801–10803. DOI: https://doi.org/10.1039/C0JM02974B

[43] K. V. Kumar, K. Preuss, Z. X. Guo, M. M. Titirici, *J. Phys. Chem. C* **2016**, *120 (32)*, 18167–18179. DOI: https://doi.org/10.1021/acs.jpcc.6b06555

[44] L. Liu, S. J. Tan, T. Horikawa, D. D. Do, D. Nicholson, J. Liu, *Adv. Colloid Interface Sci.* **2017**, *250*, 64–78. DOI: https://doi.org/10.1016/j.cis.2017.10.002